

## Programming Deformations of 3D Microstructures: Opportunities Enabled by Magnetic Alignment of Liquid Crystalline Elastomers

Shucong Li, Michael Aizenberg, Michael M. Lerch,\* and Joanna Aizenberg\*



Cite This: *Acc. Mater. Res.* 2023, 4, 1008–1019



Read Online

ACCESS |

Metrics & More

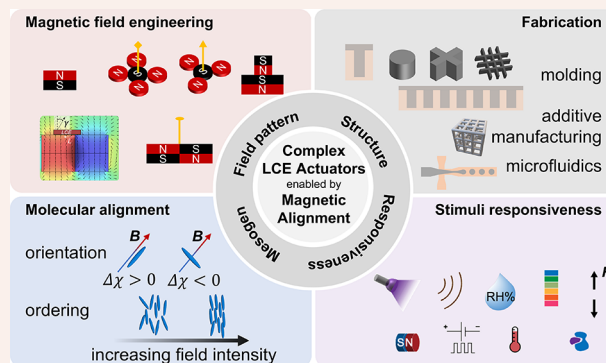
Article Recommendations

**CONSPPECTUS:** Synthetic structures that undergo controlled movement are crucial building blocks for developing new technologies applicable to robotics, healthcare, and sustainable self-regulated materials. Yet, programming motion is nontrivial, and particularly at the microscale it remains a fundamental challenge. At the macroscale, movement can be controlled by conventional electric, pneumatic, or combustion-based machinery. At the nanoscale, chemistry has taken strides in enabling molecularly fueled movement. Yet in between, at the microscale, top-down fabrication becomes cumbersome and expensive, while bottom-up chemical self-assembly and amplified molecular motion does not reach the necessary sophistication. Hence, new approaches that converge top-down and bottom-up methods and enable motional complexity at the microscale are urgently needed.

Synthetic anisotropic materials (e.g., liquid crystalline elastomers, LCEs) with encoded molecular anisotropy that are shaped into arbitrary geometries by top-down fabrication promise new opportunities to implement controlled actuation at the microscale. In such materials, motional complexity is directly linked to the built-in molecular anisotropy that can be “activated” by external stimuli. So far, encoding the desired patterns of molecular directionality has relied mostly on either mechanical or surface alignment techniques, which do not allow the decoupling of molecular and geometric features, severely restricting achievable material shapes and thus limiting attainable actuation patterns, unless complex multimaterial constructs are fabricated. Electromagnetic fields have recently emerged as possible alternatives to provide 3D control over local anisotropy, independent of the geometry of a given 3D object.

The combination of magnetic alignment and soft lithography, in particular, provides a powerful platform for the rapid, practical, and facile production of microscale soft actuators with field-defined local anisotropy. Recent work has established the feasibility of this approach with low magnetic field strengths (in the lower mT range) and comparably simple setups used for the fabrication of the microactuators, in which magnetic fields can be engineered through arrangement of permanent magnets. This workflow gives access to microstructures with unusual spatial patterning of molecular alignment and has enabled a multitude of nontrivial deformation types that would not be possible to program by any other means at the micron scale. A range of “activating” stimuli can be used to put these structures in motion, and the type of the trigger plays a key role too: directional and dynamic stimuli (such as light) make it possible to activate the patterned anisotropic material locally and transiently, which enables one to achieve and further program motional complexity and communication in microactuators.

In this Account, we will discuss recent advances in magnetic alignment of molecular anisotropy and its use in soft lithography and related fabrication approaches to create LCE microactuators. We will examine how design choices—from the molecular to the fabrication and the operational levels—control and define the achievable LCE deformations. We then address the role of stimuli in realizing the motional complexity and how one can engineer feedback within and communication between microactuator arrays fabricated by soft lithography. Overall, we outline emerging strategies that make possible a completely new approach to designing for desired sets of motions of active, microscale objects.



### INTRODUCTION

Movement is central to life, yet surprisingly difficult to coordinate.<sup>1</sup> Sophisticated biological machinery commands deformations and reconfigurations from the molecular to the macroscale, thereby achieving complex motions—from directional movement and nonreciprocal beating patterns, to combinations of elongation/contraction, twisting, bending,

**Received:** June 11, 2023

**Revised:** September 10, 2023

**Published:** September 22, 2023



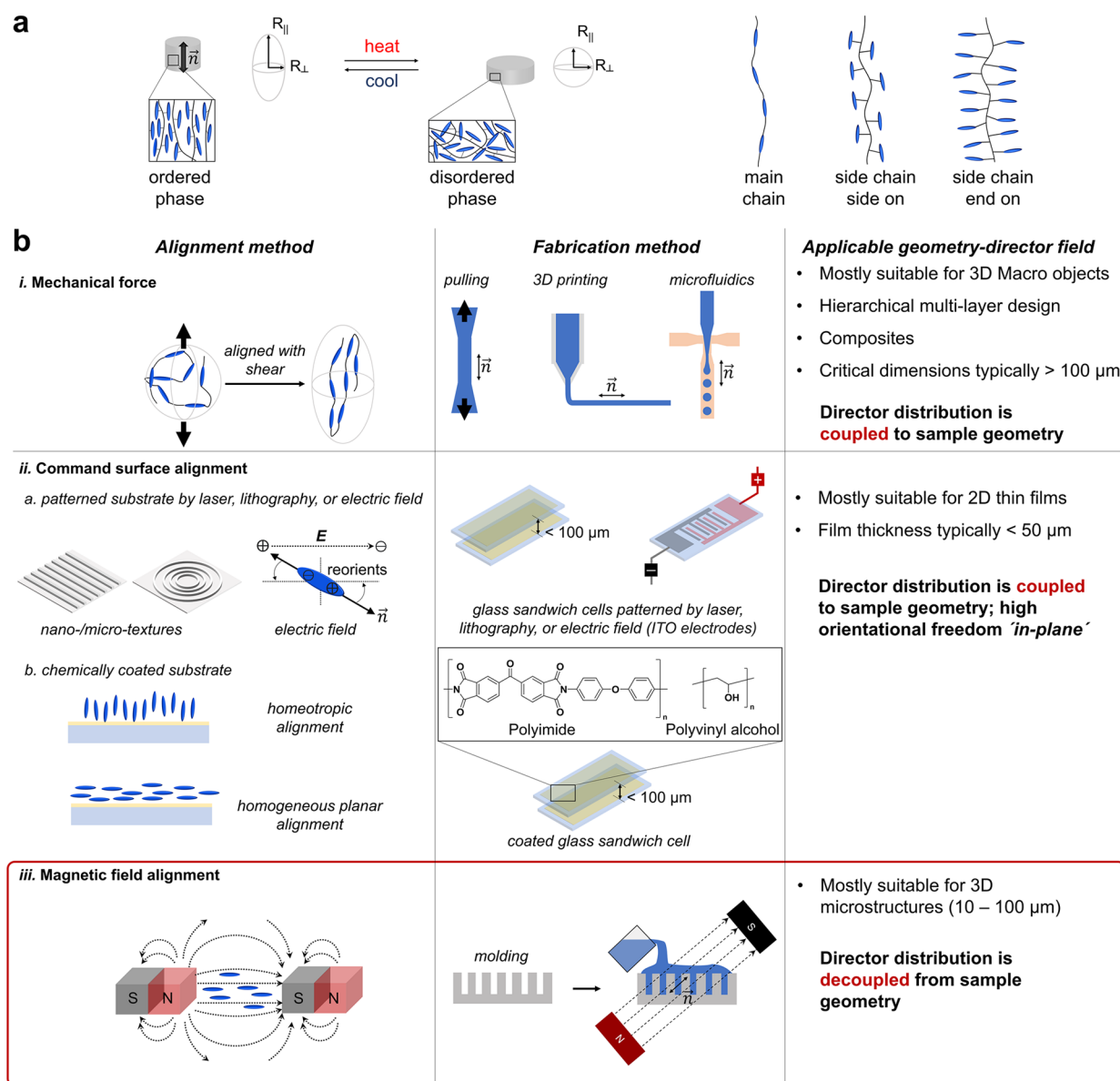


**Figure 1.** Fabrication and alignment methods for liquid crystalline elastomer (LCE) microstructures—their applicability and deficiencies: (a) An LCE undergoes a directional deformation determined by its molecular anisotropy (director  $\mathbf{n}$ ), order parameter, and network architecture. (b) Comparison of LC alignment methods and fabrication strategies through (i) mechanical force, (ii) topographical patterning, and (iii) magnetic fields. Magnetic field alignment, as a volumetric method, is decoupled from the sample geometry and allows for arbitrary choice of director orientation within molded 3D shapes (particularly at the micron scale), unlike approaches (i) and (ii).

and shearing. Developing and synthesizing soft intelligent material systems<sup>2–5</sup> mimicking this complexity promises a materials revolution in medicine and energy technologies, as well as human–machine interfaces and soft robotics, particularly for hard-to-access spaces (i.e., inside tissues), complex (unstructured) surroundings, and extreme environments.<sup>6–8</sup>

Morphing active materials, in which controlled molecular anisotropy is used to locally program deformability, constitute an emerging and promising technology. Shape deformation in this approach is not determined by a multicomponent architecture as in conventional soft actuators, but by patterning local molecular alignment across the material. Such an approach shifts the design challenges away from how to assemble a complex multimaterial composite architecture to how to program molecular and mechanical anisotropy within a single (simple) material. Recent advances in the molecular patterning

of these anisotropic materials and their actuation by directional stimuli are providing new, innovative solutions to this problem and demonstrate previously unachievable motional complexity at the microscale. The potential is tremendous: at this 1–100  $\mu\text{m}$  length-scale, an active artificial object<sup>9</sup> matches the sizes of biological structures (e.g., blood vessels: diameter 5  $\mu\text{m}$  to 25  $\mu\text{m}$ , wall thickness 0.5  $\mu\text{m}$  to 2  $\mu\text{m}$ , cell size 10–100  $\mu\text{m}$ ),<sup>10</sup> and thus has the potential to revolutionize medicine through innovations in disease reporting, structural monitoring, local and minimally invasive surgery, as well as drug delivery.

Directionality in morphing materials is commonly achieved through the use of anisotropic molecular components (e.g., liquid crystalline (LC) mesogens),<sup>11–14</sup> magnetic nanoparticles/rods with directional magnetization (polarized ferromagnetic domains),<sup>15,16</sup> or high-aspect-ratio fillers (cellulose nanofibers or glass fibers).<sup>17</sup> In all approaches, the miniaturized

soft actuator is made from a simple (host) material, which can be shaped by a molding process<sup>18–21</sup> or 3D printing.<sup>17,22</sup> Among these anisotropic materials, liquid crystalline elastomers (LCEs, Figure 1a) are of particular interest, as their deformation performance resembles muscle fibers in actuation strain, frequency, and modulus,<sup>23</sup> and can be tuned to display good biocompatibility<sup>24</sup> and degradability.<sup>25</sup> LCEs<sup>11–14</sup> are cross-linked elastomeric networks that incorporate liquid crystal mesogen units either as part of, or appended to, the polymeric backbone (Figure 1a) and can undergo programmable directional order-to-disorder transitions. For more details please refer to further reviews on LCE chemistry, synthesis, and applications.<sup>25–30</sup>

Three general alignment methods<sup>26</sup> exist (Figure 1b): alignment by mechanical force,<sup>22,31,32</sup> surface patterning (topographical or chemical),<sup>33–35</sup> and magnetic fields.<sup>18,19,36</sup> An ideal soft robot capable of multiple, sophisticated responses requires a free choice of alignment direction that is independent of the robot's shape. In practice, however, the choice of the fabrication procedure starkly limits the achievable orientations of mesogen alignment in the final sample. As detailed below, for mechanical force and surface-based aligning mechanisms, the directionality is determined by the "interface" or the "boundary" given by the sample geometry, coupling material shape and molecular patterning (Figure 1b, *i–ii*). Controlling the molecular orientation by a magnetic field, on the other hand, is a distinctly different and highly attractive method because it removes this constraint (Figure 1b, *iii*).

In this Account we will focus on the new opportunities arising when the mesogen directionality is encoded by the magnetic alignment of LCEs (bottom-up) and thus decoupled from the actuator geometry, which is independently defined by soft lithography techniques (top-down). We first briefly discuss advantages and disadvantages of commonly adopted methods, and then detail fabrication approaches based on magnetic alignment and soft lithography. We show how uniformly oriented mesogens enable rich director-determined deformations of LCE microstructures triggered by thermal actuation, and illustrate how complexity can be further increased when microstructures are fabricated in gradient and patterned magnetic fields. From there, we describe how a change from a global stimulus (such as heat) to a local and directional stimulus (such as light) changes the resulting dynamics drastically and offers multimodal and self-regulated motions enabled by opto-chemo-mechanical feedback. Further leveraging soft lithography, we highlight how the synergy between structural design (mesoscale) and director-defined anisotropic deformation of LCEs (molecular scale) opens new deformation behaviors, including collective responses in microarrays, multifunctional deformations in multisegment microstructures, and unusual modes of mechanical deformation in interconnected meta-structures.

### Magnetic Alignment in Comparison to Other Alignment Methods

Programming a desired LCE molecular anisotropy within an arbitrarily shaped micron-scale object is crucial for achieving complex movements, as they require precise control over the directionality and extent of material deformation. Various methods, such as mechanical force, command surfaces, and external fields, have been developed to achieve this (Figure 1b).

- (i) Mechanical force approach (Figure 1b, *i*), originally developed by Finkelmann,<sup>31</sup> is used as the simplest aligning

method, particularly suitable for macroscopic samples. Stretching of a partially cured non-cross-linked sample induces the mesogens to align along the stretching direction, which can be locked-in by a subsequent cross-linking step. Similarly, in 3D printing<sup>22</sup> and microfluidics,<sup>32,37</sup> the shear force of the extrusion nozzle aligns mesogens in the produced filament or droplets along the extrusion direction; therefore each printed fiber or droplet (with a typical diameter >100  $\mu\text{m}$ ) has the ability to only deform along its geometric axis. 3D printing is, thus, primarily applicable to macroscopic objects, where complex director distribution is obtained by spatially organizing the filaments into a multilayer configuration.

- (ii) Topographical alignment<sup>33–35</sup> makes use of a surface layer patterned either using a photomask, patterned electrodes for electric fields, mechanical rubbing (creating nano- or microgrooves), or inscribed by nanoscribe, to align the material conforming to the surface textures by minimizing LC elastic energy (Figure 1b, *ii.a*). Similarly, utilizing as an alignment layer a chemically coated substrate comprised of polyimide or poly(vinyl alcohol), can also induce LC alignment, either perpendicularly (known as homeotropic) or parallel to the substrate surface (known as planar; Figure 1b, *ii.b*). Additionally, splay alignment,<sup>38</sup> in which in a sandwich cell one surface is inducing homeotropic and the other surface planar orientation of the LC mesogens, is a broadly used approach to form films with enhanced bending deformations. The in-plane orientation of parallel alignment can generally be programmed without restrictions<sup>26</sup> and be patterned by photoalignment with high spatial resolution.<sup>33</sup> Since the alignment layer's ability to instill directional order decreases rapidly with increasing distance from the surface, both topographical and chemical methods are limited to producing only thin films (typically <50  $\mu\text{m}$ -thick, with notable exceptions<sup>39</sup>).
- (iii) In contrast, external fields *acting on the bulk of the material* allow for larger sample thickness (up to millimeter and centimeter within a reasonable field strength and alignment time) and less constraint with respect to achievable alignment orientations, decoupling material anisotropy from material geometry (Figure 1b, *iii*). *Importantly, a rather weak magnetic field (<~0.1 Tesla) is sufficient to orient the mesogens into ordered mesophases, usually nematic, as it is applied to small molecules within the (often molten) liquid crystalline monomer mixture (typically placed in a mold that determines any desired final 3D shape), before locking it in during polymerization.*

While mechanical and surface alignment approaches are most widely practiced, using magnetic fields, we argue, has been underappreciated, though it provides an extremely powerful and convenient approach for patterning molecular anisotropy within complex 3D shapes (as opposed to thin films, fibers or droplets), especially at the microscale.<sup>18–21,40,41</sup> In principle, the extent of alignment (order parameter) and its directionality can be defined precisely at each point (voxel) of the 3D volume, independently of the sample geometry.

### Magnetic Alignment (Bottom-up) Meets Soft Lithography (Top-down)<sup>18–20</sup>

Magnetic alignment of mesogens seamlessly integrates with fabrication approaches such as replica molding, microfluidics, or additive manufacturing to generate intricate 3D (micro)-

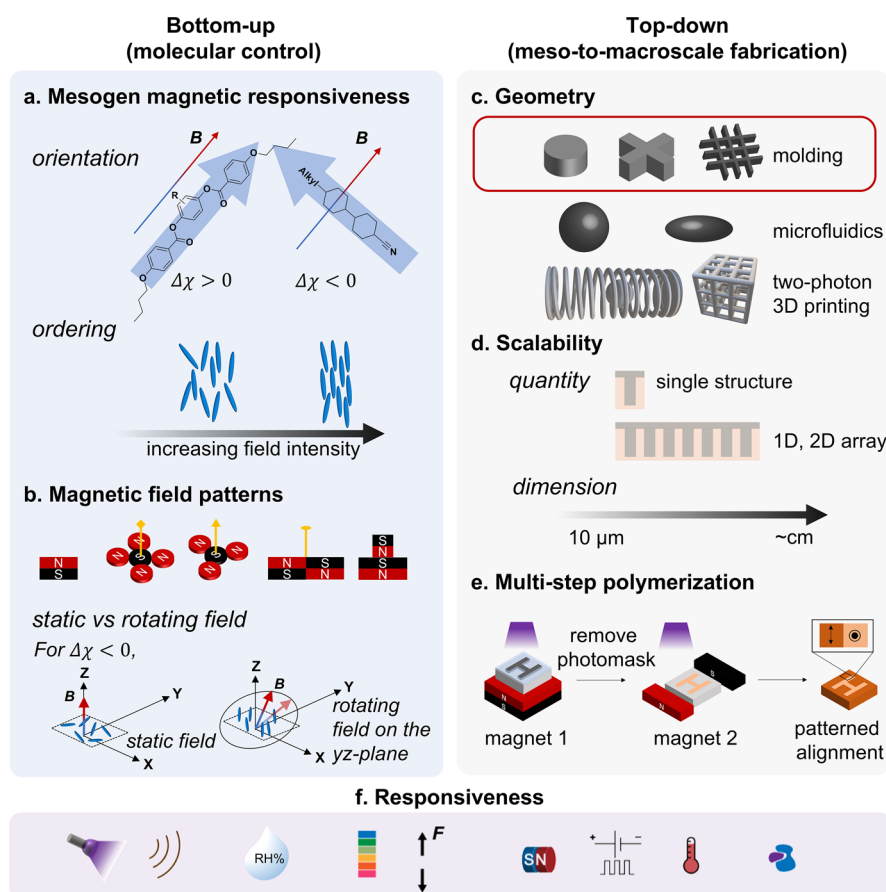


**Figure 2.** Magnetic alignment of LC mesogens enables arbitrary director orientations in LCEs, thereby significantly expanding achievable microactuator deformations. (a) The molecular structure of the mesogens and magnetic field strength affect the mesogens' propensity for alignment. (b) Various magnetic field patterns are accessible through changing arrangements of magnets. (c) Magnetic field alignment is compatible with a wide range of geometries and manufacturing methods. (d) Fabrication is easily scalable to multiple shapes and (micro)structure arrays. (e) Region-specific alignment by multistep polymerization and discontinuous director fields. (f) Through chemical modifications, LCEs can be actuated by various stimuli.

structures, in which one can independently customize geometry and the local molecular alignment (Figure 2).

At the molecular level, LC mesogen chemistry and network architecture shape the relationship between the alignment director and the resulting deformation. Most aromatic calamitic mesogens display a positive diamagnetic susceptibility ( $\Delta\chi = \chi_{\parallel} - \chi_{\perp}$ ,  $\Delta\chi > 0$ ) and tend to align parallel to the magnetic field  $\mathbf{B}$  (Figure 2a, left), often in practically easily accessible magnetic field strengths (e.g., commercial Neodymium magnets) in their monomeric, liquid state prior to polymerization.<sup>14,42–44</sup> This anisotropic diamagnetic susceptibility stems from a zero-net spin and dispersed electron distribution associated with the delocalized charge, for example, from phenyl rings. In contrast, purely alicyclic mesogens display negative diamagnetic anisotropy  $\Delta\chi < 0$  (Figure 2a, right),<sup>45</sup> which causes them to orient randomly within a 2D plane. Directional alignment can be then obtained by rotating magnetic fields, the so-called precision alignment method.<sup>45</sup> The time frame of reorientation depends on the size of the object and occurs within a second for small molecules.<sup>42</sup> It is worth noting that diamagnetic mesogens have a relatively low magnetic susceptibility, which may pose limitations for applications requiring extremely weak magnetic field strengths. To address this limitation, incorporation of ferro- or ferrimagnetic materials or doping rare earth metal ions into liquid crystal mesogens has been explored.<sup>46,47</sup> The network architecture matters too; calamitic mesogens are commonly

used as main chain, side-chain side-on, and side-chain end-on, and can adopt a prolate or oblate ellipsoid chain configuration (Figure 1a, right). Note that the alignment of oligomers or polymers requires much higher magnetic field strengths and longer relaxation time than the alignment of small molecules, and therefore it is most practical to use the magnetic field to orient LC monomers before polymerization.

The magnetic field itself can be tuned by the arrangement of magnets; a variety of configurations with resulting patterned magnetic fields are accessible with little effort (Figure 2b). In addition, the correlation of magnetic field strength and resulting order parameter of the LCE opens the possibility to program not only local director, but also magnitude of deformation response, constituting, in effect, grayscale encoding, by changing the position and orientation of the sample in the magnetic field.

At the fabrication level, the material can be made into any shape through various techniques including simple replica molding: a negative mold is filled with LC monomers, heated to the isotropic state and slowly cooled within a static magnetic field below the  $T_{NI}$  followed by polymerization.<sup>18–20</sup> In principle, any<sup>21</sup> arbitrary patterned mold generated by soft lithography, two-photon additive manufacturing or 3D printing can be used (Figure 2c). An arbitrary director field may be encoded within a molded object, whose size can range from  $\sim 10 \mu\text{m}$  (size limited due to the conflicting effect of the surface alignment induced by the walls of the mold<sup>19</sup>) to centimeter scale, and both free-

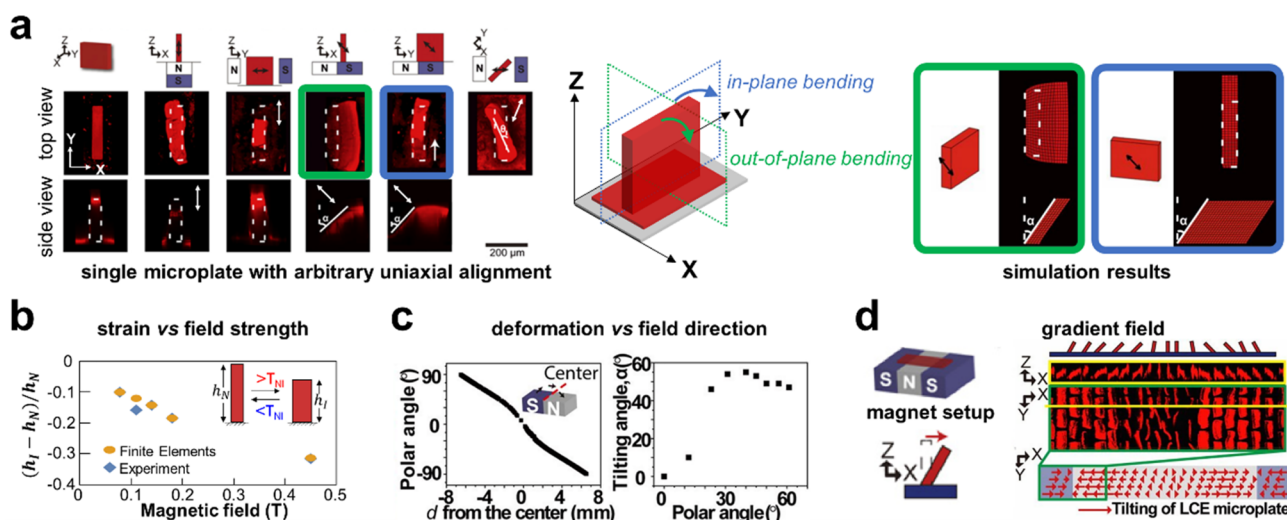


**Figure 3.** New types of deformations result from the combination of magnetic alignment and soft lithography: (a) Fluorescence confocal microscopy images of deforming single LCE microplates ( $250 \times 50 \times 200 \mu\text{m}$ ) with different director orientations, when heated  $>125^\circ\text{C}$  (left), and corresponding finite element simulations for the in-plane and out-of-plane bending (right). (b) Correlation of magnetic field strength during fabrication and the resulting extent of mechanical deformation for a  $z$ -aligned microplate, in experiment and theory. (c) The magnetic field direction can be continuously modulated by changing position of the sample or arrangement of permanent magnets, affecting the tilting angle. Left: Calculated polar angles (COMSOL) of the director as a function of the distance  $d$  from the magnet center. Right: Experimentally measured microplate tilting angles confirming this trend. (d) Gradual change in tilting angles is experimentally illustrated in an array of microplates. Images adapted with permission from refs 19, 41. Copyright (2018) National Academy of Sciences and Copyright (2021) Wiley, respectively.

standing objects or arrays of structures can be formed (Figure 2d).<sup>19,41,48,49</sup> For discontinuous director fields, multistep polymerization is recommended, in which different regions of the object are encoded with different magnetic director fields (Figure 2e). Furthermore, this multistep approach enables facile access to complex 3D architectures at the sub- $100 \mu\text{m}$  scale, which are not possible to make by other techniques.

At the operational level, patterned LCE 3D objects are not limited to solely thermal actuation (Figure 2f). Chemical modification of LCE mesogens or the backbone and incorporation of additional responsive species, can induce LCE deformation upon application of stimuli other than temperature, including light, sound, humidity, pH, electric or magnetic fields, small molecules, solvent-induced swelling, or chemical reactions.

### Director-Determined Deformation of LCE Microactuators—Magnetic Field Engineering

In 2018,<sup>19</sup> our group programmed microstructures with an arbitrary uniaxial director orientation in 3D by simply changing the relative orientation of the mold and the static magnetic field. Note that molecular anisotropy and microstructure geometry are fully decoupled, which enables director-structure configurations that are not accessible by other aligning methods. For example, as shown in Figure 3a,<sup>19</sup> an extremely rich deformation palette can be achieved from side-chain side-on LCE microstructures of a simple plate geometry: expansion/shrinkage along different directions, bending, or twisting. Of particular note is the in-plane tilting, which is a mechanically strongly disfavored type of deformation—the in-plane bending stiffness (Figure 3a, blue box) of the microplate is  $\sim 24$ -times higher than that of the out-of-plane bending (Figure 3a, green box) for a  $250 \times 50 \times 200 \mu\text{m}$  plate in this example. Moreover, the twisting is as unusual as it is interesting, since it creates chirality from an *a priori non chiral* microstructure.<sup>19</sup> We note that such atypical deformations originate from the order-to-disorder transition of the underlying molecular assembly and are considered strongly

energetically unfavorable, if at all possible, in common passive structures and force-based deformation mechanisms (e.g., magnetic-field-triggered elastomers with embedded ferromagnetic nanoparticles<sup>15,16</sup> or arrays of passive microstructures embedded in actuable hydrogel<sup>50</sup>).

The strength of the local magnetic field directly correlates with the LCE's local scalar order parameter  $S$  and hence magnitude of response. Such grayscale encoding provides a powerful means to pattern the local response and expand the range of possible deformations. We have shown<sup>41</sup> that the shrinkage strain of  $z$ -aligned microplates along the  $z$ -axis,  $\epsilon_z$  ( $\epsilon_z = (h_I - h_N)/h_N$ , where  $h_N$  and  $h_I$  are the microplate heights in the nematic and isotropic phases, respectively) monotonically increases with the intensity of the magnetic field (Figure 3b). When using multiple magnets,<sup>19,41</sup> one can create magnet assemblies of different geometries and symmetries to encode local field information. For example, when two permanent magnets are placed adjacent with north (N) and south (S) pole upward, the magnetic field on the surface will tilt gradually: at the center where the magnets meet, the orientation will be horizontal, and with distance ( $d$ ) from the center, this angle will tilt upright (Figure 3c). Taking advantage of these features makes it possible to create arrays of microstructures, in which each member will have a slightly different director orientation; for instance, this can easily be observed in a molded array of microstructures placed during the fabrication process on top of three magnets (Figure 3d). Upon thermal actuation, at one side of the array, pillars bend along the  $x$ -axis, in the middle of the array pillars elongate, and at the other side they bend along the  $x$ -axis in opposite direction. Such continuous modulation of directionality across the sample could facilitate screening for ideal conditions, encoding phase differences or wave-like behaviors in arrays. With these advantages, the magnetic alignment method is far superior in its versatility compared to other alignment methods, allowing an almost “dial-in” approach to encoding mechanical responses of LCE actuators.

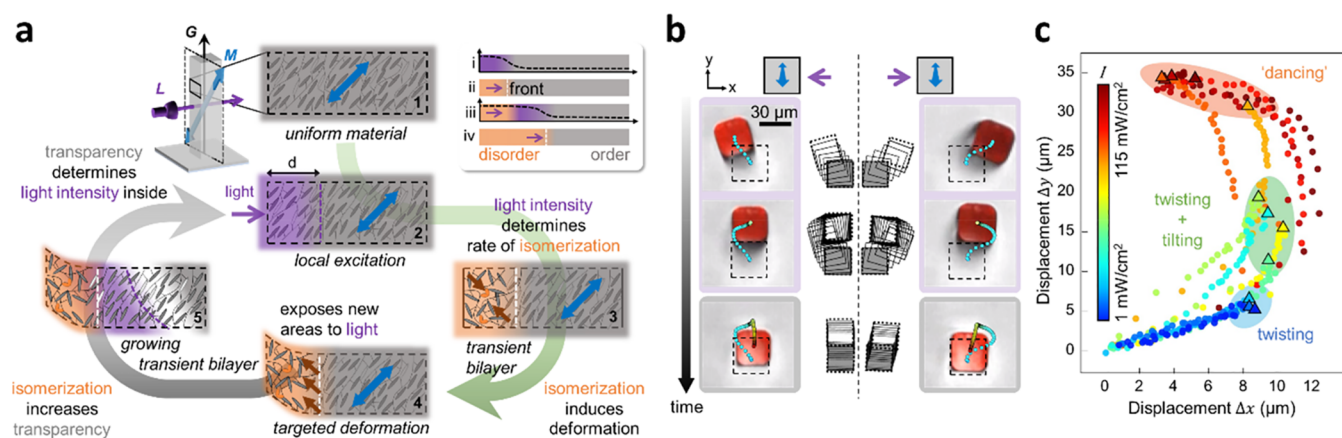


**Figure 4.** A directional stimulus such as light can create transient, dynamically changing bimorphs of activated and nonactivated regions. (a) Illustration of the underlying opto-chemo-mechanical feedback in an LCE micropost with noncollinear geometric axis (G), molecular anisotropy (M), and light direction (L) (1). As light penetrates (2), only a part of the material becomes activated (3), which deforms along the director (4). The deformation changes the subsequent activation step (5), which is made possible by induced transparency (inset top right, in which activation (i and ii) makes the material partially transparent to the activating light, causing deeper penetration and activation (iii and iv)). Depending on the light intensity, the feedback loop can either be completed (gray flow arrow, high intensity), or stopped at the initial deformation (green flow arrow, low intensity). (b) Out-of-plane UV-irradiation of a square micropost ( $30 \times 30 \times 150 \mu\text{m}$ ) with tilted director alignment causes a characteristic and finely tunable power stroke. Depending on the light-direction, the same pillar can sway into opposite directions. (c) Motion trajectory as a function of light intensity. Images adapted with permission from ref 48. Copyright (2022) Springer Nature.

### Multimodal Deformation—Adding a Directional Stimulus

Typically, calamitic mesogens form thermotropic liquid crystals;<sup>14</sup> that is, the LCE deforms with temperature along the director. Incorporation of stimuli-responsive molecular units into the elastomers can provide responsiveness to other external stimuli (Figure 4). For example, molecular photoswitches can be used as light-sensitive cross-linkers.<sup>51,52</sup> Upon light-exposure, these molecules either exert a photomechanical force, pulling on the polymer backbone and disrupting the molecular order,<sup>53</sup> act as photothermal heaters,<sup>54</sup> facilitating the thermal phase transition,<sup>27</sup> or act as photoplasticizers to introduce free volume from the continuous oscillating isomerizations.<sup>55</sup> Similarly, use of mesogens with a strong dipole or embedding mesogens in a dielectric matrix allows deformation of the LCE within a changing electric field.<sup>56</sup> Further means of activation include humidity,<sup>57</sup> chemicals,<sup>58</sup> and magnetic fields<sup>59</sup> (for LCEs with incorporated superparamagnetic nanoparticles).

Much more complex behaviors can be achieved, if the stimulus is applied directionally, allowing for sequential activation as the stimulus (i.e., light) propagates through the material over time.<sup>48,60,61</sup> While many reported thin film LCE systems are generally activated globally due to either their inherent thinness or a low concentration of absorbing species,<sup>51</sup> thicker samples or samples with a higher concentration of light absorbent effectively generate a bimorph structure upon illumination, which consists of an activated region (where the light penetrates into) and a nonactivated region (where light does not reach). The resulting bimorph resembles closely a traditional multilayer composite, with a crucial difference originating from the microstructure being made of a *single material*: light activation is usually reversible as thus are the activation and transient bimorph formation. For a microstructure (e.g., a micropost) with a director aligned along its principal axis, phototropic behavior results, in which the structure bends toward the light.<sup>19</sup> Related (isotropic) systems of gold nanoparticle-containing hydrogel beams behave similarly.<sup>62</sup> If the director orientation, however, is different from the beam's axis, the deformation behavior changes

significantly and various light direction-dependent deformations result: bending toward light, bending away from light, and twisting in clock- and counterclockwise directions, notably all from the same structure and same material throughout.<sup>48,63</sup> Complex multimaterial constructs and hybrid structures would be needed, if traditional fabrication approaches were applied.

### Self-Regulated Complex Deformation—Enabling Propagating Stimulus

In some cases, photoactivation of the light-responsive species causes induced transparency,<sup>60,61</sup> when the activated and isomerized photoswitch absorbs little at the wavelength of activation and thus allows the light to penetrate deeper into the material. What results is an intensity-dependent traveling front of order–disorder transition across the material. This effect has been well-known for highly absorbing thin films, in which upon irradiation, the film first bends toward light (as only one side becomes activated), followed by a reversal of motion, as activation propagates through the film and finally activates it globally.<sup>60,61</sup> For nonflat 3D structures with off-axis director alignment, this leads to the emergence of complex motion trajectories controlled by an intricate opto-chemo-mechanical feedback loop (Figure 4a), in which the activated region reshapes and becomes increasingly complex because of the continuous reorientation of the microstructure and local director upon deformation in the static light field.<sup>48</sup> Take for example a square micropost with tilted director alignment subjected to out-of-plane irradiation: initial transient bimorph formation causes the activated slab to shear, inducing a twisting deformation of the post. Once twisting motion ensues, new facets of the post are exposed and others shadowed, which changes the activated region and thus influences the subsequent movement. What results is a stroke-like deformation trajectory that resembles the movement of cilia,<sup>64</sup> which is direction- (Figure 4b) and light-intensity-dependent (Figure 4c).

The scope of possible and *programmable* deformations and actuation trajectories of the same microstructure is practically limitless, even for simple architectures and uniform (but oblique) director alignments. One can capture and predict

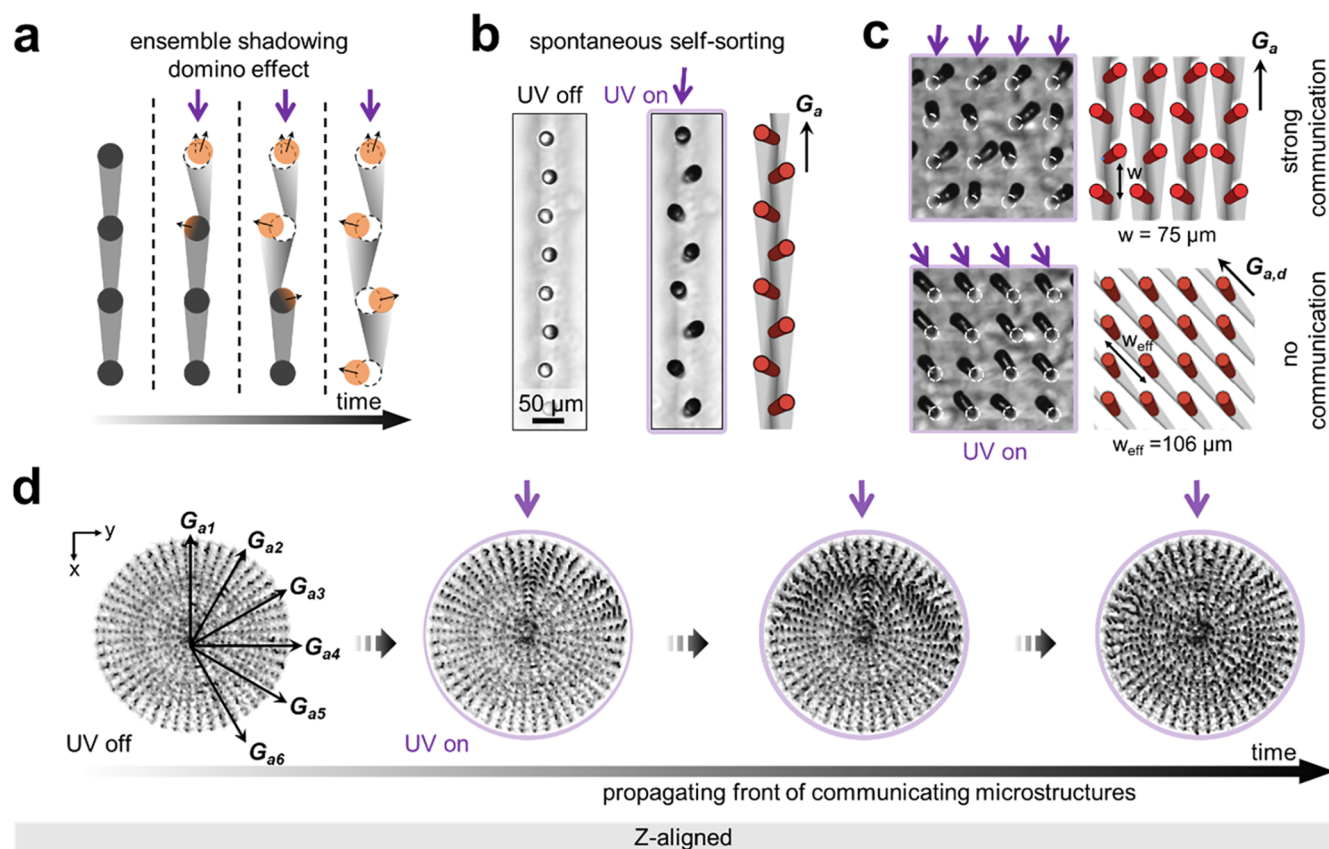


**Figure 5.** Emergence of communication and coordinated movements in arrays of microactuators. (a) Illustration of how shadowing causes a domino effect in ensembles of LCE microposts when slight off-axis illumination exposes the subsequent pillar unevenly. (b) Experimental observation (left) and modeling (right) of the resulting zigzag self-sorted pattern. (c) Experiment (left) and modeling (right), showing interpillar communication when illuminated along the array (top), and absence thereof when illuminated in a diagonal direction (bottom). (d) In more complex cases, programmable “metachronal” waves emerge. Images adapted with permission from ref 48. Copyright (2022) Springer Nature.

these deformation trajectories quantitatively with theoretical models.<sup>48,63</sup> Interesting next steps will be to expand these studies to more complex material geometries, in which various segments have a locally different director alignment with respect to their segmental principal axes. Theoretical predictions suggest a wide range of microstructure behaviors including stirring, catching, and releasing.<sup>48</sup>

We emphasize again that the oblique director alignment, which is necessary for these nonreciprocal, stroke-like deformations, is only attainable through magnetic alignment of the mesogens. Surface alignment is generally limited to either homeotropic or planar alignment and to thinner samples. Use of mechanical force to align mesogens in a tilted fashion within pillars is nontrivial at microscale and has not been demonstrated. The use of 3D-printing and shear forces for alignment along the 3D-printed thread is also not feasible at the 10–100 μm size range described above.

### Collective Deformation—Microarray Engineering by Soft Lithography

The combination of facile fabrication of arrays of microstructures through magnetic alignment and molding together with the complex deformations arising from directional activation open new avenues for creating ensembles of microstructures with coordinated deformation behaviors.<sup>48</sup> In the biological context, coupled motion of arrays of microactuators—take for instance metachronal waves in cilia carpets<sup>64</sup>—are essential for directional transport and highly

interesting for soft robotics. The light-induced deformation trajectory of each LCE micropost in a closely packed multipillar system influences the light exposure of neighboring structures enabling interpillar communication. As a result, in strings of microposts, an unusual (if not unprecedented) self-sorting behavior is observed (Figure 5). For example, by engineering a slight misalignment between the illumination direction and the string axis, the off-axis bending of the first pillar causes asymmetric exposure of the second pillar and its out-of-string bending, which further triggers a cascade of “self-avoiding” actions progressing along the string like a domino (Figure 5a,b). The communication is highly direction-dependent and sensitive to interpillar distances, which causes interesting self-sorting behaviors in 2D arrays, illuminated along different symmetry axes (Figure 5c).

For larger 2D arrays of microposts more complex traveling wave patterns can be programmed by varying local molecular alignment, interpillar distance, or irradiation direction. As a result, each deforming pillar contributes to an overall “metachronal” wave across the array (Figure 5d). Enabled by computational modeling and based on the versatility, programmability, and the vast design space for individual and collective motions, many user-defined applications for such soft robotic carpets become possible. In particular, these ensemble motions, when coupled with the stroke-like behavior of each individual pillar, may allow for locally controlled “walking”-type movements, or controlled transport more generally, as currently already being explored with ferromagnetic elastomers.<sup>65,66</sup>

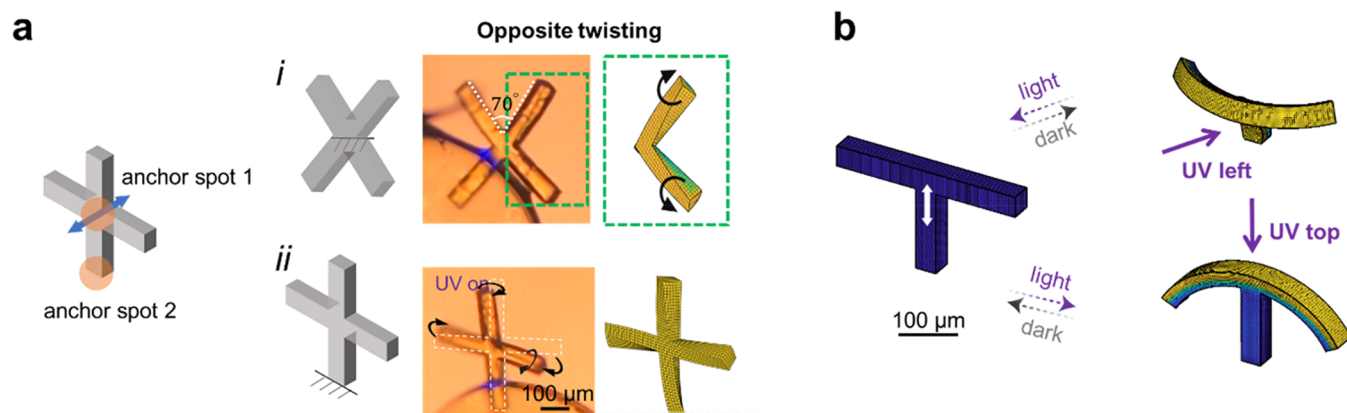


**Figure 6.** Multimodal deformations in jointed compositionally uniform microactuators. (a) Cross-shaped LCE microactuator with different anchoring spots displays different deformation behaviors: (i) when center-anchored, symmetric inward and outward twisting can be invoked for different arms, (ii) while with asymmetric anchoring of one arm, the twisting of the vertical arm couples to the twisting/rotation of the horizontal segment, enabling amplification of the sway motion. Experiments, center; simulations, right. (b) Diverse motions can be also obtained by changing illumination directions (simulations). Photoactuation is depicted by the blue-to-yellow transition. Images adapted with permission from ref 48. Copyright (2022) Springer Nature.

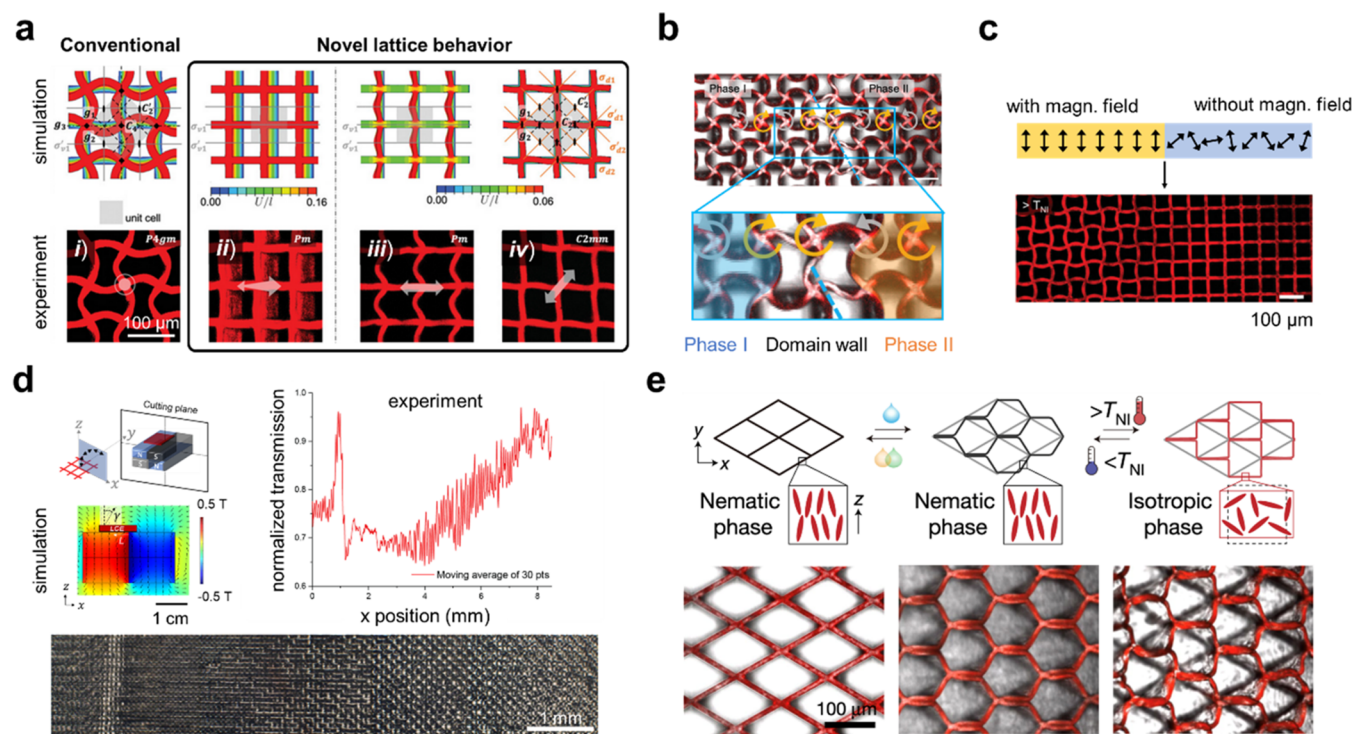


**Figure 7.** Deformations of base-attached cellular LCE microstructures. (a) Different director alignment causes different deformations both in simulation (top) and experiment (bottom). (b) Domain walls (indicated by the blue dashed line) in the form of a second order buckling pattern in a first-order buckling square lattice. (c) Two-step polymerization enables encoding area-specific buckling patterns. (d) Optical microscopy images (bottom) and transmitted light intensity profile (right) at  $T = 135\text{ }^{\circ}\text{C} > T_{NI}$  by an LCE square lattice with mesogenic director gradually changing from  $-20^{\circ}$  to  $90^{\circ}$ . (e) Combination of multiple stimuli for deforming z-aligned diamond-shaped cellular LCE structures. Images adapted with permission from refs 41, 49. Copyright (2021) Wiley and Copyright (2021) Springer Nature, respectively.

### Multisegment Multimodal Deformation—Engineering Geometry by Soft Lithography

In the above sections, we introduced how a single micropost can be programmed with various asymmetric mechanical deformations by choice of (magnetic) director alignment and irradiation conditions. Figure 6 further showcases how symmetry breaking in molded *jointed* shapes can enable *structural communication* to unlock unusual mechanical deformations. For example, in LCE structures with uniform director orientation, molded in the form

of V-, X-, or T-shapes, as well as “multihand” configurations, each segment will have a different relative orientation between its own principal symmetry axis and the bulk director, causing each segment to simultaneously undergo its own (different) deformation. For instance, an X-shape LCE with uniform oblique alignment can display twisting of opposite handedness for the two diagonals when center-anchored, or sway motion when base-anchored (Figure 6a),<sup>48</sup> promising applications as multifunctional soft robots in versatile environments. Similarly,



irradiating a T-shaped actuator from different sides will cause it to undergo different motions, as illustrated by finite element simulations (Figure 6b).

### Expanding to Mechanical Metamaterials—Cellular Lattice Engineering by Soft Lithography

Spatial confinement of the deforming structure, from anchoring or connection to neighboring structures, strongly influences preprogrammed deformations and enables new, previously inaccessible deformation modes. For example, base-attached cellular geometries, readily accessible with soft lithography, such as a square lattice with magnetically induced molecular alignment, display various types of cell-to-cell or node-to-node communications and directional patterns of buckling (Figure 7a), including (i) isotropic buckling, (ii) global shearing (opposite from the director tilt), (iii) single direction buckling (vertical plates undergoing buckling and horizontal plates under high tension), and (iv) square-to-diamond lattice transformation. *In contrast, conventional mechanical metamaterials usually undergo only isotropic buckling, unless multilayer composites are used, which are impractical at the microscale.*<sup>67</sup> The points of connectivity modulate communication between cells as is illustrated by a z-aligned staggered square lattice (Figure 7b): upon phase transition, a new buckling pattern, in which adjacent nodes rotate in alternating manner to avoid local stress concentration, appears. If domains of such patterns are out-of-phase (depicted in orange or gray in Figure 7b), second-order buckling is seen at domain walls.

Nonuniform, local or gradient molecular alignments across the sample give rise to area-selective deformations. For example, if only a section of the lattice has molecular alignment produced by multistep polymerization of the masked region (see Figure 2e), upon heating the aligned part undergoes buckling and the nonaligned part remains inactive (Figure 7c).<sup>41</sup> If the director is spatially varied across the lattice, the resulting deformations in the metamaterial spatially modulate the lattice's light transmission profile. Figure 7d shows an LCE strip with mesogenic director gradually changing from  $-20^\circ$  to  $90^\circ$  by positioning the sample off-center in the magnetic field. The lattice appears bright at  $T < T_{NI}$ , yet above  $T_{NI}$  the transmitted light shows a dark-bright-dark-bright pattern following the spatially varying lattice deformation. Hence, magnetic alignment of LCEs brings new opportunities for designing unexplored deformation modes in mechanical metamaterials with lattice geometries.

Instead of light or heat, LCE microstructures (and in fact any polymeric structures<sup>68</sup>) can be deformed through solvent-induced swelling and capillary assembly (Figure 7e).<sup>49</sup> For example, cellular LCE structures when exposed to acetone undergo isotropic swelling of the transiently softened elastomer and concomitant buckling of the walls. As the solvent evaporates, the receding meniscus in the lattice voids exerts a force that allows assembly of the softened walls into new structures. Due to the glassy state of the LCE polymer (conformational kinetic trapping) and the interfacial adhesion, the assembled lattice stays stable even after drying. The assembled structure can be disassembled in a solvent mixture, that softens the polymer and introduces drastic swelling to peel apart the assembled plates.<sup>49</sup> Figure 7e illustrates this for a base-attached diamond lattice that undergoes solvent-induced topological transformations into a hexagonal lattice, useful for tunable acoustic, optical, electrical, and mechanical properties, as well as heat, fluid and particle transport.<sup>49</sup> If the mesogens in the LCE are magnetically aligned, these assembled lattices will

undergo further deformations upon heating, as exemplified by the heat-triggered hexagonal-to-brick transformation, giving rise to a cascade of different transformations of the same structure by applying different stimuli.

### In Context—Comparison to Deformations of Magnetic Elastomers

LCEs are *active* materials that can respond to external stimuli and provide substantial directional actuation strain of up to 400%.<sup>11</sup> We emphasize again that the magnetic field is only used for the alignment of the LC monomers during fabrication, but not as a stimulus for the actuation of the created LCE microstructures. In contrast, (hard-)magnet (soft) elastomers<sup>15</sup> (that is, polymeric host matrices with embedded well-dispersed polarized ferromagnetic nano/microparticles), are *passive* and the magnetic field acts as an external force on the ferromagnetic domains defined by the local polarization. In the latter case, mechanically unfavored deformation modes—thin plate twisting or bending along the long axis, global shearing of honeycomb lattices, as described here—are not observed. Moreover, magnetic elastomers are intrinsically limited by their stretchability and the local force strength obtained through the magnet, leading to a low deformation strain of  $<25\%$ ,<sup>15,16</sup> compared to 400% achievable by the LCEs. As a result, a “normal”, out-of-plane bending of such magnetic elastomers is employed most often.<sup>16</sup> We further note that magnetic elastomers show superfast actuation ( $<0.1$  s),<sup>15</sup> while LCEs often exhibit longer response times.

## CONCLUSION AND OUTLOOK

Magnetic alignment of liquid crystalline mesogens *at low magnetic field strength prior to polymerization*, as described in this review, enables free programming of LC director orientations, many of which have previously been impossible to achieve by other methods, such as surface alignment or alignment by mechanical stretching. The newly gained freedom in controlling both the local direction and magnitude of active material deformations directly translates to vastly expanded possibilities for designing more complex actuation patterns in easy-to-fabricate single-material soft robots, particularly at the microscale. In this Account, we described the principles of magnetic alignment, suitable LC mesogens, and resulting advantages. We then discussed examples of thermally triggered active mechanical deformations of microstructures and lattices and showed that the magnetic alignment approach is scalable and therefore compatible with mass-production of micro- to macroscale actuators of desired 3D shapes. We then showed how directional stimuli, i.e., light, enable completely new, previously unthinkable user-programmable motions, including an unlimited range of actuation trajectories that the same microstructure can exhibit as a function of temperature, light direction, and light intensity, when the orientation of the director oblique to the microstructure geometrical axis is encoded by magnetic alignment. In addition, solvent-controlled swelling—softening/deswelling—stiffening and elastocapillary assembly are demonstrated as means to further expand deformational complexity, particularly in cellular lattices.<sup>41,49</sup> The described approaches, each on their own, but even more so when combined, provide a range of breakthroughs in materials science and enable highly complex, programmable mechanical deformations displayed by a single material, introducing ways for communication and propagation of patterns within free-standing, attached, and cellular arrays of microstructures.

Underlying opto-chemo-mechanical feedback<sup>48</sup> gives rise to self-organization of coordinated motion and holds promise for much more complex ensemble behaviors. Our proof-of-concept studies just barely scratch the surface of the advanced potential applications these approaches bring into the realm of what is possible.

Ultimately, the motional freedom opened by magnetic alignment provides a fundamentally new approach to rational design of user-controlled deformations based on simple, chemically versatile polymers. Beyond the presented materials, many other liquid crystalline mesogens, backbone chemistry, and LCE architectures<sup>69</sup> remain to be explored and their capacity to align within magnetic fields and yield deformations further studied. These polymer networks may not need to be fixed: chemical reprogramming of the local director based on dynamic covalent networks<sup>25,70</sup> that go beyond erasing or reprocessing warrants further exploration. In addition, such adaptable networks may aid in fabrication and combination of multiple components.<sup>71,72</sup> Moreover, other stimuli such as electric fields, mechanical force, chemical concentration gradients, humidity, or sound may be used for triggering (local) phase transitions and may be combined in additive or orthogonal fashion to enable multiple material responses, signal integration, and rudimentary computation.

## ■ AUTHOR INFORMATION

### Corresponding Authors

**Michael M. Lerch** – John A. Paulson School of Engineering and Applied Sciences, Harvard University, Cambridge, Massachusetts 02138, United States; Stratingh Institute for Chemistry, University of Groningen, 9747 AG Groningen, The Netherlands; [orcid.org/0000-0003-1765-0301](https://orcid.org/0000-0003-1765-0301); Email: [m.m.lerch@rug.nl](mailto:m.m.lerch@rug.nl)

**Joanna Aizenberg** – Department of Chemistry and Chemical Biology and John A. Paulson School of Engineering and Applied Sciences, Harvard University, Cambridge, Massachusetts 02138, United States; [orcid.org/0000-0002-2343-8705](https://orcid.org/0000-0002-2343-8705); Email: [jaiz@seas.harvard.edu](mailto:jaiz@seas.harvard.edu)

### Authors

**Shucong Li** – Department of Chemistry and Chemical Biology, Harvard University, Cambridge, Massachusetts 02138, United States; Department of Mechanical Engineering, Massachusetts Institute of Technology, Cambridge, Massachusetts 02139, United States

**Michael Aizenberg** – John A. Paulson School of Engineering and Applied Sciences, Harvard University, Cambridge, Massachusetts 02138, United States; [orcid.org/0000-0002-2901-7012](https://orcid.org/0000-0002-2901-7012)

Complete contact information is available at:

<https://pubs.acs.org/10.1021/accountsmr.3c00101>

### Notes

The authors declare no competing financial interest.

### Biographies

**Shucong Li** received her PhD in Chemistry at Harvard University on polymeric reconfigurable microstructures. She is now a postdoctoral associate at MIT, focusing on hydrogel phase separations, magnetic elastomers, additive manufacturing, and applications in healthcare and energy harvesting systems.

**Michael Aizenberg** is a senior staff scientist at Harvard University John A. Paulson School of Engineering and Applied Sciences. He received his PhD in Organometallic Chemistry from the Weizmann Institute of Science. After doing his postdoctoral research at MIT, he spent a decade in the fragrance and pharmaceutical sectors of chemical industry, following which he joined materials chemistry research efforts at Harvard. His research is centered on developing self-regulated and advanced catalytic materials.

**Michael M. Lerch** is an assistant professor at the Stratingh Institute for Chemistry at the University of Groningen, working on self-regulated and autonomous soft materials. He holds a PhD in Organic and Supramolecular Chemistry. As a postdoctoral fellow at Harvard University, he worked on liquid crystalline elastomer microactuators.

**Joanna Aizenberg** is Amy Smith Beryson Professor of Materials Science and Professor of Chemistry and Chemical Biology at Harvard University. She received her PhD in Structural Biology from the Weizmann Institute of Science, following which she was a postdoctoral fellow at Harvard University and a member of the Bell Laboratories Technical Staff. Throughout her career, she has made a number of pioneering contributions in the field of bioinspired materials chemistry. Aizenberg is a member of the National Academy of Science, National Academy of Engineering, American Philosophical Society, and American Academy of Arts and Sciences.

## ■ ACKNOWLEDGMENTS

This material is based upon work supported by the Department of Energy under Award DE-SC0005247 (polymer design and characterization) and by the Department of Defense, Army Research Office under Award W911NF-17-1-0351 (self-regulated optical devices). M.M.L. was supported by The Netherlands Organization for Scientific Research (NWO VENI Grant, VI.Veni.202.158).

## ■ REFERENCES

- (1) Lancia, F.; Ryabchun, A.; Katsonis, N. Life-like Motion Driven by Artificial Molecular Machines. *Nat. Rev. Chem.* **2019**, *3* (9), 536–551.
- (2) Kaspar, C.; Ravoo, B. J.; van der Wiel, W. G.; Wegner, S. V.; Pernice, W. H. P. The Rise of Intelligent Matter. *Nature* **2021**, 594 (7863), 345–355.
- (3) Zhang, X.; Chen, L.; Lim, K. W. H.; Gonuguntla, S.; Lim, K. W. H.; Pranantyo, D.; Yong, W. P.; Yam, W. J. T.; Low, Z.; Teo, W. J.; Nien, H. P.; Loh, Q. W.; Soh, S. The Pathway to Intelligence: Using Stimuli-Responsive Materials as Building Blocks for Constructing Smart and Functional Systems. *Adv. Mater.* **2019**, *31* (11), e1804540.
- (4) Lerch, M. M.; Grinthal, A.; Aizenberg, J. Viewpoint: Homeostasis as Inspiration—Toward Interactive Materials. *Adv. Mater.* **2020**, *32* (20), 1905554.
- (5) Xia, X.; Spadaccini, C. M.; Greer, J. R. Responsive Materials Architected in Space and Time. *Nat. Rev. Mater.* **2022**, *7* (9), 683–701.
- (6) Whitesides, G. M. Soft Robotics. *Angew. Chem., Int. Ed.* **2018**, *57* (16), 4258–4273.
- (7) Rus, D.; Tolley, M. T. Design, Fabrication and Control of Soft Robots. *Nature* **2015**, *521* (7553), 467–475.
- (8) Li, M.; Pal, A.; Aghakhani, A.; Pena-Francesch, A.; Sitti, M. Soft Actuators for Real-World Applications. *Nat. Rev. Mater.* **2022**, *7* (3), 235–249.
- (9) Palagi, S.; Fischer, P. Bioinspired Microrobots. *Nat. Rev. Mater.* **2018**, *3* (6), 113–124.
- (10) Hardin, J.; Lodolce, J. P. *Becker's World of the Cell*, 10th ed.; Pearson: Harlow, England, 2021.
- (11) Ohm, C.; Brehmer, M.; Zentel, R. Liquid Crystalline Elastomers as Actuators and Sensors. *Adv. Mater.* **2010**, *22* (31), 3366–3387.

- (12) White, T. J.; Broer, D. J. Programmable and Adaptive Mechanics with Liquid Crystal Polymer Networks and Elastomers. *Nat. Mater.* **2015**, *14* (11), 1087–1098.
- (13) Warner, M.; Terentjev, E. M. *Liquid Crystal Elastomers*, revised ed.; Clarendon Press: Oxford, 2007.
- (14) *Handbook of Liquid Crystals*, 2nd ed.; Goodby, J. W., Collings, P. J., Kato, T., Tschierske, C., Gleeson, H., Raynes, P., Eds.; Wiley-VCH: Weinheim, 2014.
- (15) Kim, Y.; Yuk, H.; Zhao, R.; Chester, S. A.; Zhao, X. Printing Ferromagnetic Domains for Untethered Fast-Transforming Soft Materials. *Nature* **2018**, *558* (7709), 274–279.
- (16) Kim, Y.; Zhao, X. Magnetic Soft Materials and Robots. *Chem. Rev.* **2022**, *122* (5), 5317–5364.
- (17) Sydney Gladman, A.; Matsumoto, E. A.; Nuzzo, R. G.; Mahadevan, L.; Lewis, J. A. Biomimetic 4D Printing. *Nat. Mater.* **2016**, *15* (4), 413–418.
- (18) Buguin, A.; Li, M. H.; Silberzan, P.; Ladoux, B.; Keller, P. Micro-Actuators: When Artificial Muscles Made of Nematic Liquid Crystal Elastomers Meet Soft Lithography. *J. Am. Chem. Soc.* **2006**, *128* (4), 1088–1089.
- (19) Yao, Y.; Waters, J. T.; Shneidman, A. V.; Cui, J.; Wang, X.; Mandsberg, N. K.; Li, S.; Balazs, A. C.; Aizenberg, J. Multiresponsive Polymeric Microstructures with Encoded Predetermined and Self-Regulated Deformability. *Proc. Natl. Acad. Sci. U.S.A.* **2018**, *115* (51), 12950–12955.
- (20) Yang, H.; Buguin, A.; Taulemesse, J.-M.; Kaneko, K.; Mery, S.; Bergeret, A.; Keller, P. Micron-Sized Main-Chain Liquid Crystalline Elastomer Actuators with Ultralarge Amplitude Contractions. *J. Am. Chem. Soc.* **2009**, *131* (41), 15000–15004.
- (21) Ni, B.; Liu, G.; Zhang, M.; Tatoulian, M.; Keller, P.; Li, M. H. Customizable Sophisticated Three-Dimensional Shape Changes of Large-Size Liquid Crystal Elastomer Actuators. *ACS Appl. Mater. Interfaces* **2021**, *13* (45), 54439–54446.
- (22) del Pozo, M.; Sol, J. A. H. P.; Schenning, A. P. H. J.; Debije, M. G. 4D Printing of Liquid Crystals: What's Right for Me? *Adv. Mater.* **2022**, *34* (3), 2104390.
- (23) Thomsen, D. L.; Keller, P.; Naciri, J.; Pink, R.; Jeon, H.; Shenoy, D.; Ratna, B. R. Liquid Crystal Elastomers with Mechanical Properties of a Muscle. *Macromolecules* **2001**, *34* (17), 5868–5875.
- (24) Turiv, T.; Krieger, J.; Babakhanova, G.; Yu, H.; Shiyankovskii, S. V.; Wei, Q. H.; Kim, M. H.; Lavrentovich, O. D. Topology Control of Human Fibroblast Cells Monolayer by Liquid Crystal Elastomer. *Sci. Adv.* **2020**, *6* (20), eaaz6485.
- (25) Saed, M. O.; Gablier, A.; Terentjev, E. M. Exchangeable Liquid Crystalline Elastomers and Their Applications. *Chem. Rev.* **2022**, *122* (5), 4927–4945.
- (26) Herbert, K. M.; Fowler, H. E.; McCracken, J. M.; Schlafmann, K. R.; Koch, J. A.; White, T. J. Synthesis and Alignment of Liquid Crystalline Elastomers. *Nat. Rev. Mater.* **2022**, *7* (1), 23–38.
- (27) Liu, D.; Broer, D. J. *Responsive Polymer Surfaces*; Wiley-VCH: Newark, 2017.
- (28) Bisoyi, H. K.; Li, Q. Liquid Crystals: Versatile Self-Organized Smart Soft Materials. *Chem. Rev.* **2022**, *122* (5), 4887–4926.
- (29) Wang, Y.; Liu, J.; Yang, S. Multi-Functional Liquid Crystal Elastomer Composites. *Appl. Phys. Rev.* **2022**, *9* (1), 011301.
- (30) Huang, S.; Huang, Y.; Li, Q. Photodeformable Liquid Crystalline Polymers Containing Functional Additives: Toward Photomanipulatable Intelligent Soft Systems. *Small Struct.* **2021**, *2* (9), 2100038.
- (31) Küpfer, J.; Finkelmann, H. Nematic Liquid Single Crystal Elastomers. *Macromol. Rapid Commun.* **1991**, *12* (12), 717–726.
- (32) Ohm, C.; Kapernaum, N.; Nonnenmacher, D.; Giesselmann, F.; Serra, C.; Zentel, R. Microfluidic Synthesis of Highly Shape-Anisotropic Particles from Liquid Crystalline Elastomers with Defined Director Field Configurations. *J. Am. Chem. Soc.* **2011**, *133* (14), 5305–5311.
- (33) Ware, T. H.; McConney, M. E.; Wie, J. J.; Tondiglia, V. P.; White, T. J. Voxellated Liquid Crystal Elastomers. *Science* **2015**, *347* (6225), 982–984.
- (34) Aharoni, H.; Xia, Y.; Zhang, X.; Kamien, R. D.; Yang, S. Universal Inverse Design of Surfaces with Thin Nematic Liquid Elastomer Sheets. *Proc. Natl. Acad. Sci. U.S.A.* **2018**, *115* (28), 7206–7211.
- (35) Guo, Y.; Shahsavan, H.; Sitti, M. 3D Microstructures of Liquid Crystal Networks with Programmed Voxellated Director Fields. *Adv. Mater.* **2020**, *32* (38), 2002753.
- (36) Brehmer, M.; Zentel, R.; Wagenblast, G.; Siemsmeyer, K. Ferroelectric Liquid-Crystalline Elastomers. *Macromol. Chem. Phys.* **1994**, *195* (6), 1891–1904.
- (37) Liu, M.; Han, X.; Nah, S. H.; Wu, T.; Wang, Y.; Feng, L.; Wu, L.; Yang, S. Switching Chirality in Arrays of Shape-Reconfigurable Spindle Microparticles. *Adv. Mater.* **2023**, *35* (31), 2303009.
- (38) Mol, G. N.; Harris, K. D.; Bastiaansen, C. W. M.; Broer, D. J. Thermo-Mechanical Responses of Liquid-Crystal Networks with a Splayed Molecular Organization. *Adv. Funct. Mater.* **2005**, *15* (7), 1155–1159.
- (39) McCracken, J. M.; Hoang, J. D.; Herman, J. A.; Lynch, K. M.; White, T. J. Millimeter-Thick Liquid Crystalline Elastomer Actuators Prepared by-Surface-Enforced Alignment. *Adv. Mater. Technol.* **2023**, *8* (13), 2202067.
- (40) Ni, B.; Liu, G.; Zhang, M.; Keller, P.; Tatoulian, M.; Li, M. H. Large-Size Honeycomb-Shaped and Iris-Like Liquid Crystal Elastomer Actuators. *ACS Chem.* **2022**, *4* (3), 847–854.
- (41) Li, S.; Librandi, G.; Yao, Y.; Richard, A. J.; Schneider-Yamamura, A.; Aizenberg, J.; Bertoldi, K. Controlling Liquid Crystal Orientations for Programmable Anisotropic Transformations in Cellular Microstructures. *Adv. Mater.* **2021**, *33* (42), 2105024.
- (42) Moore, J. S.; Stupp, S. I. Orientation Dynamics of Main-Chain Liquid Crystal Polymers. 1. Synthesis and Characterization of the Mesogen. *Macromol.* **1987**, *20* (2), 273–281.
- (43) Kimura, T. Study of the Effect of Magnetic Fields on Polymeric Materials and Its Application. *Polym. J.* **2003**, *35* (11), 823–843.
- (44) Shin, J.; Kang, M.; Tsai, T.; Leal, C.; Braun, P. V.; Cahill, D. G. Thermally Functional Liquid Crystal Networks by Magnetic Field Driven Molecular Orientation. *ACS Macro Lett.* **2016**, *5* (8), 955–960.
- (45) Pohl, L.; Eidenschink, R.; Krause, J.; Weber, G. Nematic Liquid Crystals with Positive Dielectric and Negative Diamagnetic Anisotropy. *Phys. Lett. A* **1978**, *65* (2), 169–172.
- (46) Podoliak, N.; Buchnev, O.; Buluy, O.; D'Alessandro, G.; Kaczmarek, M.; Reznikov, Y.; Sluckin, T. J. Macroscopic Optical Effects in Low Concentration Ferronematics. *Soft Matter* **2011**, *7* (10), 4742–4749.
- (47) Binnemans, K.; Galyametdinov, Y. G.; Van Deun, R.; Bruce, D. W.; Collinson, S. R.; Polishchuk, A. P.; Bikchantaev, I.; Haase, W.; Prosvirin, A. V.; Tinchurina, L.; Litvinov, I.; Gubajdullin, A.; Rakhmatullin, A.; Uytterhoeven, K.; Van Meervelt, L. Rare-Earth-Containing Magnetic Liquid Crystals. *J. Am. Chem. Soc.* **2000**, *122* (18), 4335–4344.
- (48) Li, S.; Lerch, M. M.; Waters, J. T.; Deng, B.; Martens, R. S.; Yao, Y.; Kim, D. Y.; Bertoldi, K.; Grinthal, A.; Balazs, A. C.; Aizenberg, J. Self-Regulated Non-Reciprocal Motions in Single-Material Microstructures. *Nature* **2022**, *605* (7908), 76–83.
- (49) Li, S.; Deng, B.; Grinthal, A.; Schneider-Yamamura, A.; Kang, J.; Martens, R. S.; Zhang, C. T.; Li, J.; Yu, S.; Bertoldi, K.; Aizenberg, J. Liquid-Induced Topological Transformations of Cellular Microstructures. *Nature* **2021**, *592* (7854), 386–391.
- (50) Kim, P.; Zarzar, L. D.; He, X.; Grinthal, A.; Aizenberg, J. Hydrogel-Actuated Integrated Responsive Systems (HAIRS): Moving towards Adaptive Materials. *Curr. Opin. Solid State Mater. Sci.* **2011**, *15* (6), 236–245.
- (51) Pilz da Cunha, M.; van Thoor, E. A. J.; Debije, M. G.; Broer, D. J.; Schenning, A. P. H. J. Unravelling the Photothermal and Photo-mechanical Contributions to Actuation of Azobenzene-Doped Liquid Crystal Polymers in Air and Water. *J. Mater. Chem. C* **2019**, *7* (43), 13502–13509.
- (52) Bisoyi, H. K.; Li, Q. Light-Driven Liquid Crystalline Materials: From Photo-Induced Phase Transitions and Property Modulations to Applications. *Chem. Rev.* **2016**, *116* (24), 15089–15166.

- (53) Barrett, C. J.; Mamiya, J.; Yager, K. G.; Ikeda, T. Photo-Mechanical Effects in Azobenzene-Containing Soft Materials. *Soft Matter* **2007**, *3* (10), 1249–1261.
- (54) Gelebart, A. H.; Vantomme, G.; Meijer, E. W.; Broer, D. J. Mastering the Photothermal Effect in Liquid Crystal Networks: A General Approach for Self-Sustained Mechanical Oscillators. *Adv. Mater.* **2017**, *29* (18), 1606712.
- (55) Liu, D.; Broer, D. J. New Insights into Photoactivated Volume Generation Boost Surface Morphing in Liquid Crystal Coatings. *Nat. Commun.* **2015**, *6* (1), 8334.
- (56) Fowler, H. E.; Rothmund, P.; Keplinger, C.; White, T. J. Liquid Crystal Elastomers with Enhanced Directional Actuation to Electric Fields. *Adv. Mater.* **2021**, *33* (43), 2103806.
- (57) De Haan, L. T.; Verjans, J. M. N.; Broer, D. J.; Bastiaansen, C. W. M.; Schenning, A. P. H. J. Humidity-Responsive Liquid Crystalline Polymer Actuators with an Asymmetry in the Molecular Trigger That Bend, Fold, and Curl. *J. Am. Chem. Soc.* **2014**, *136* (30), 10585–10588.
- (58) Gelebart, A. H.; Mulder, D. J.; Vantomme, G.; Schenning, A. P. H. J.; Broer, D. J. A Rewritable, Reprogrammable, Dual Light-Responsive Polymer Actuator. *Angew. Chem., Int. Ed.* **2017**, *56* (43), 13436–13439.
- (59) Winkler, M.; Kaiser, A.; Krause, S.; Finkelmann, H.; Schmidt, A. M. Liquid Crystal Elastomers with Magnetic Actuation. *Macromol. Symp.* **2010**, *291–292* (1), 186–192.
- (60) Corbett, D.; Warner, M. Linear and Nonlinear Photoinduced Deformations of Cantilevers. *Phys. Rev. Lett.* **2007**, *99* (17), 174302.
- (61) Corbett, D.; Xuan, C.; Warner, M. Deep Optical Penetration Dynamics in Photobending. *Phys. Rev. E* **2015**, *92* (1), 13206.
- (62) Qian, X.; Zhao, Y.; Alsaïd, Y.; Wang, X.; Hua, M.; Galy, T.; Gopalakrishna, H.; Yang, Y.; Cui, J.; Liu, N.; Marszewski, M.; Pilon, L.; Jiang, H.; He, X. Artificial Phototropism for Omnidirectional Tracking and Harvesting of Light. *Nat. Nanotechnol.* **2019**, *14* (11), 1048–1055.
- (63) Waters, J. T.; Li, S.; Yao, Y.; Lerch, M. M.; Aizenberg, M.; Aizenberg, J.; Balazs, A. C. Twist Again: Dynamically and Reversibly Controllable Chirality in Liquid Crystalline Elastomer Microposts. *Sci. Adv.* **2020**, *6* (13), eaay5349.
- (64) Gilpin, W.; Bull, M. S.; Prakash, M. The Multiscale Physics of Cilia and Flagella. *Nat. Rev. Phys.* **2020**, *2*, 74–88.
- (65) Gu, H.; Boehler, Q.; Cui, H.; Secchi, E.; Savorana, G.; De Marco, C.; Gervasoni, S.; Peyron, Q.; Huang, T.-Y.; Pane, S.; Hirt, A. M.; Ahmed, D.; Nelson, B. J. Magnetic Cilia Carpets with Programmable Metachronal Waves. *Nat. Commun.* **2020**, *11* (1), 2637.
- (66) Ren, Z.; Zhang, M.; Song, S.; Liu, Z.; Hong, C.; Wang, T.; Dong, X.; Hu, W.; Sitti, M. Soft-Robotic Ciliated Epidermis for Reconfigurable Coordinated Fluid Manipulation. *Sci. Adv.* **2022**, *8* (34), eabq2345.
- (67) Khan, M.; Shan, S.; Aizenberg, J.; Noorduyn, W. L.; Bertoldi, K.; Kang, S. H. Buckling-Induced Reversible Symmetry Breaking and Amplification of Chirality Using Supported Cellular Structures. *Adv. Mater.* **2013**, *25* (24), 3380–3385.
- (68) Pokroy, B.; Kang, S. H.; Mahadevan, L.; Aizenberg, J. Self-Organization of a Mesoscale Bristle into Ordered, Hierarchical Helical Assemblies. *Science* **2009**, *323* (5911), 237–240.
- (69) Xu, Y.; Dupont, R. L.; Yao, Y.; Zhang, M.; Fang, J.-C.; Wang, X. Random Liquid Crystalline Copolymers Consisting of Prolate and Oblate Liquid Crystal Monomers. *Macromol.* **2021**, *54* (12), 5376–5387.
- (70) Webber, M. J.; Tibbitt, M. W. Dynamic and Reconfigurable Materials from Reversible Network Interactions. *Nat. Rev. Mater.* **2022**, *7* (7), 541–556.
- (71) Chen, L.; Bisoyi, H. K.; Huang, Y.; Huang, S.; Wang, M.; Yang, H.; Li, Q. Healable and Rearrangeable Networks of Liquid Crystal Elastomers Enabled by Diselenide Bonds. *Angew. Chem., Int. Ed.* **2021**, *60* (30), 16394–16398.
- (72) Huang, S.; Shen, Y.; Bisoyi, H. K.; Tao, Y.; Liu, Z.; Wang, M.; Yang, H.; Li, Q. Covalent Adaptable Liquid Crystal Networks Enabled by Reversible Ring-Opening Cascades of Cyclic Disulfides. *J. Am. Chem. Soc.* **2021**, *143* (32), 12543–12551.